

## A New Method for Evaluating the Conformations and Normal Modes of Macromolecule Vibrations with a Reduced Force Field. 2. Application to Nonplanar Distorted Metal Porphyrins

Esko Unger,<sup>†</sup> Michael Beck,<sup>†</sup> Robert J. Lipski,<sup>†</sup> Wolfgang Dreybrodt,<sup>‡</sup> Craig J. Medforth,<sup>‡</sup> Kevin M. Smith,<sup>‡</sup> and Reinhard Schweitzer-Stenner<sup>\*,†,§</sup>

FB1-Institute of Experimental Physics, University of Bremen, 28359 Bremen, Germany;

Department of Chemistry, University of California, Davis, California 95616; and Department of Chemistry, University of Puerto Rico, San Juan, Puerto Rico 00931-3334

Received: June 21, 1999; In Final Form: September 9, 1999

We have developed a novel method for molecular mechanics calculations and normal-mode analysis. It is based on symmetry of local units that constitutes the given molecule. Compared with general valence force field calculations, the number of free parameters is reduced by 40–80% in our procedure. It was found to reproduce very well the vibrational frequencies and mode compositions of aromatic compounds and porphyrins, as shown by comparison with DFT calculations. A slightly altered force field obtained from Ni(II) porphyrin was then used to calculate the structure and the normal modes of several meso-substituted Ni(II) porphyrins which are known to be subject to significant ruffling and/or saddling distortions. This method satisfactorily reproduces their nonplanar structure and Raman band frequencies in the natural abundance and isotopic derivative spectra. The polarization properties of bands from out-of-plane modes are in accordance with the predicted nonplanar distortions. Moreover, we found that some of the modes below 800 cm<sup>-1</sup> which appear intense in the Raman spectra contain considerable contributions from both in-plane and out-of-plane vibrations, so that the conventional mode assignments become questionable. We also demonstrate that the intensity and polarization of some low-frequency Raman bands can be used as a (quantitative) marker to elucidate type and magnitude of out-of-plane distortions. These were recently shown to affect heme groups of hemoglobin, myoglobin, and, in particular, of cytochrome *c*.

### Introduction

Interest has recently been expressed in the possible biological significance of the nonplanar distortions observed for porphyrins in protein structures.<sup>1</sup> Nonplanar porphyrins were observed in a large number of protein crystal structures<sup>2</sup> and also by spectroscopic studies (e.g. in the dispersion of depolarization ratios).<sup>3</sup> Studies of nonplanar model porphyrins indicate that distortions modulate some properties of biochemical relevance, e.g., axial ligand affinities,<sup>4</sup> electron transfer rates,<sup>5</sup> and the oxidation potential of various cytochromes.<sup>6</sup>

In the absence of external forces and steric crowding of the porphyrin substituents, the macrocycle exhibits *D*<sub>4h</sub> symmetry, because this corresponds to the lowest energy of the  $\pi$ -electronic system. The symmetry of porphyrins in heme proteins, however, is generally lowered by interactions with amino acid residues, by the asymmetric arrangement of its substituents, and by endogenous and exogenous ligands.<sup>7</sup> A recent study, utilizing a novel decomposition method, showed that the most common macrocycle distortions are of symmetry type B<sub>1u</sub> (ruffling), B<sub>2u</sub> (saddling), and to a minor extent of type A<sub>2u</sub> (doming).<sup>8</sup> The type and magnitude of these distortions differ for various heme

groups, but they are often conserved for heme groups in proteins with the same biological function (e.g. for cytochromes *c*).<sup>6</sup>

In order to explore the parameters determining the porphyrin conformation and to model the distorted heme groups, a variety of synthetic metalloporphyrins with different central metal ions have been investigated. The porphyrin macrocycle was found to be quite flexible, and its structure is influenced by the metal–nitrogen distance (core size) and by substituent steric interactions. Comparison of UV–vis and Raman spectra of these porphyrins revealed that the frequencies of some Raman lines designated as core-size markers, as well as those of the Q and B absorption bands, are correlated with the degree of macrocycle nonplanarity.<sup>9</sup> Roughly speaking, the magnitude of out-of-plane distortions was found to increase with increasing bulkiness of the peripheral substituents and with smaller metals which favor a reduced core size. The porphyrin conformation also depends on its environment and aggregation state. Meso-substituted copper(II) tetraphenylporphyrin (CuTPP), for instance, crystallizes in a strongly ruffled and slightly saddled conformation,<sup>10</sup> as does the corresponding nickel(II) compound (NiTPP).<sup>11</sup> In organic solution, however, CuTPP was shown to be (quasi)-planar,<sup>12</sup> while NiTPP coexists in two conformations, from which the nonplanar conformation, which is very likely identical or similar to that obtained in the crystal, is the more stabilized one.<sup>13</sup> For porphyrins with more (bulky) substituents the structure is probably less dependent on environmental parameters and the core size. Octaethyltetraphenylporphyrin with different metals crystallizes in essentially the same conforma-

\* Author to whom all correspondence should be addressed. Phone: 787-764-0000-(2417). Fax: 787-763-6899. E-mail: stenner@web.uprr.pr. Address for correspondence: Department of Chemistry, University of Puerto Rico, San Juan, PR 00931-3334.

<sup>†</sup> University of Bremen.

<sup>‡</sup> University of California, Davis.

<sup>§</sup> University of Puerto Rico.

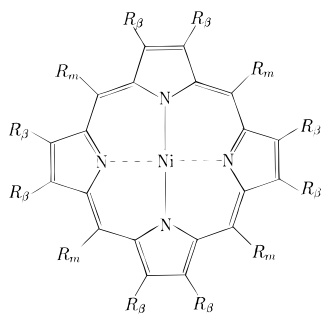


**Figure 1.** Structure of the porphyrins investigated: (a) NiTetP:  $R_\beta = \text{H}$ ,  $R_m = \text{ethyl}$ ; (b) NiTMeP:  $R_\beta = \text{H}$ ,  $R_m = \text{methyl}$ ; (c) NiTPP:  $R_\beta = \text{H}$ ,  $R_m = \text{phenyl}$ ; (d) NiTiPrP:  $R_\beta = \text{H}$ ,  $R_m = \text{isopropyl}$ ; (e) NiTiBuP:  $R_\beta = \text{H}$ ,  $R_m = \text{tert-butyl}$ ; (f) NiOETPP:  $R_\beta = \text{ethyl}$ ,  $R_m = \text{phenyl}$ .

tion,<sup>14</sup> and there is evidence that NiOETPP has a similar or even identical structure in solution.<sup>3b</sup> As a general rule, porphyrins with small substituents are more flexible and their conformations are therefore more sensitive to environmental changes. This is strongly supported by the results of the present paper.

In a preceding study, we developed a novel method for consistent molecular mechanics and normal-mode calculations using an empirical force field expressed in terms of local symmetry coordinates.<sup>15</sup> This method utilized local symmetry within the compartments of the analyzed molecule to reduce the number of force constants, but did not require global symmetry. This allowed us to calculate normal modes even for highly asymmetric porphyrins by employing fewer free parameters than available frequency values. Moreover, relatively large molecules could also be treated in this fashion. In the present study, we use this new method to explore the structural and spectroscopic properties of a series of nickel(II) *meso*-substituted porphyrins in organic solution (cf. Figure 1). Additionally, we have investigated NiOETPP, a standard model compound for fully substituted porphyrins. As shown earlier by crystallographic studies, Raman data and by molecular mechanics calculations, all these porphyrins are nonplanar distorted.<sup>4,9</sup> For the very first time we have now calculated the normal modes of these porphyrins by explicitly including the distortions of these macrocycles.

In the spectroscopic part of the paper, we focus on the analysis of B-band-excited Raman spectra, providing Raman lines arising from Franck–Condon active modes which are predominantly enhanced by A-term scattering. Generally, only those modes which maintain the symmetry of the molecule can be Franck–Condon active. In  $D_{4h}$  symmetry, this only holds for  $A_{1g}$  modes.<sup>3</sup> In the presence of an out-of-plane distortion, however, additional modes may become Raman active.  $B_{1u}$  modes, for instance, become Raman active if the macrocycle is affected by ruffling ( $B_{1u}$ ) distortions. In the following study, we show that polarized Raman lines assignable to  $B_{1u}$  modes appear in the spectra of all *meso*-substituted porphyrins, and some of these are quite intense. Evidently, in noncoordinating solvents, these porphyrins exist in a nonplanar conformation with some ruffling component, in accordance with predictions from molecular mechanics calculations. Additionally, the absence of Raman lines corresponding to  $B_{2u}$  modes suggests the lack of a saddling distortion. Tetraphenylporphyrins, however, are exceptions from this rule. This is not surprising, because NiTPP and even CuTPP very likely exhibit a small saddling distortion.<sup>10</sup>

An unambiguous assessment of these distortions cannot be obtained solely by information provided by Raman spectra. For example, two types of out-of-plane distortions are required to

cause a dispersion of the depolarization ratio and the types of distortions cannot be uniquely determined without further data and considerations. Moreover, in-plane and out-of-plane distortions cannot be discriminated without utilizing further information about the porphyrin structure obtained by other techniques. The frequencies of some core size marker bands can be used to determine the degree of nonplanarity,<sup>4,9,14</sup> while the type of distortion cannot be obtained. Thus, the assignment of the Raman bands by normal-coordinate analysis arising from out-of-plane modes provides valuable structural information.

The molecular structures of various *meso*-substituted porphyrins have previously been investigated by Jentzen et al.<sup>9</sup> On the basis of molecular mechanics calculations, these authors predicted that all of these porphyrins are ruffled and that the degree of ruffling increases with the size of the substituents. To verify their results, the calculated conformations were compared with corresponding structures determined by X-ray crystallography. Our molecular mechanics results confirm their findings for the tetraalkylporphyrins.

In addition, we also investigated the structure and the Raman spectra of highly nonplanar NiOETPP. Its structure was previously calculated by Shelnutt et al.<sup>4</sup> and was found to be saddled. Its Raman lines were first assigned by Stichternath et al. based on polarized resonance Raman, FT-Raman, and FT-IR spectra of the natural abundance and the derivative with deuterated phenyl groups.<sup>16</sup> Somewhat later, Piffat et al.<sup>17</sup> suggested an assignment based on a normal-mode analysis for a planar model configuration. Both studies suggested basically the same assignment but differ with respect to a few Raman lines. We will refer to this point in detail in the Results and Discussion section. Contrary to Piffat et al.,<sup>17</sup> our normal-mode calculation is performed for the saddled conformation predicted by our molecular mechanics calculation that is nearly identical to that obtained from X-ray crystallographic data.

Finally, we have some comments concerning the mode assignments made in the above studies. For proper assignments it is necessary to know which mode corresponds to which Raman line and to have a reasonable criterion for the mode designation. In  $D_{4h}$  symmetry, the Raman active modes can be classified due to four representations of the group, namely  $A_{1g}$ ,  $A_{2g}$ ,  $B_{1g}$ , and  $B_{2g}$ . Furthermore, it is common to distinguish between macrocycle modes and substituent modes, although this discrimination is not necessarily appropriate because mode eigenvectors often exhibit contributions from both. The nomenclature of the macrocycle modes is based on the criterion of maximal similarity with the modes of nickel(II) octaethylporphyrin (NiOEP), which is used as a reference system. The classification of modes for porphyrins exhibiting lower symmetry is more difficult, especially because the mode eigenvectors of nonplanar porphyrins can exhibit both in- and out-of-plane contributions. Although it seems impractical to apply the nomenclature for NiOEP to these complicated systems, the Raman spectra of distorted porphyrins are generally very similar to those having  $D_{4h}$  symmetry and suggest that their lines result from modes with similar eigenvectors. Indeed, our results for low-symmetry porphyrins reveal these modes to be very similar to those in the high-symmetry case. It is therefore desirable to use the NiOEP nomenclature also for distorted porphyrins, as this has already been done for some prominent Raman lines in several studies.<sup>3,9,17</sup>

We have employed a special procedure which provides a strictly quantitative criterion for the mode designation. For a given compound, we first calculate the normal modes of a corresponding planar model molecule, in which all substituents

are replaced by a point mass of 12 u. This has been done because the first atom of the substituents is always a carbon. The normal-mode compositions and frequencies of the “simple” model system turned out to be very similar to those of the “complete” molecule in which the substituents were included. In the second step, we compare the simple and complete systems. Because the model only consists of the 37 macrocycle atoms, those modes of the complete molecule being most similar to the modes of the simple system can be reasonably defined as the macrocycle modes. The degree of similarity is measured by the dot product of the normalized mass-weighted Cartesian displacement vectors of the two modes compared as described by Unger et al.<sup>15</sup> By this procedure, we were able to distinguish between macrocycle and substituent modes, with all of the macrocycle modes being definitively assigned. The method also provides a strict criterion to distinguish between in- and out-of-plane modes.

## Materials and Methods

**Preparation.** Nickel(II) and copper(II) tetraphenylporphyrin (NiTPP and CuTPP) were purchased from Porphyrin Products (Logan, UT) and were further purified by liquid chromatography using CS<sub>2</sub> (Aldrich, HPLC grade) as the mobile phase (column 1 × 10 cm<sup>2</sup>; Silica 32-63, 60 Å, ICN Biomedicals). The homogeneity of the sample was checked by thin-layer chromatography using Kieselgel with fluorescence indicator F254 (Merck). Samples of nickel(II) octaethyltetraphenylporphyrin (NiOETPP),<sup>4</sup> nickel(II) tetramethylporphyrin (NiTMeP), nickel(II) tetraethylporphyrin (NiTEtP), nickel(II) tetraisopropylporphyrin (NiTiPrP), and nickel(II) tetra-*tert*-butylporphyrin (NiTtBuP)<sup>9</sup> were synthesized as described in the literature. The samples were spectroscopically probed either in CS<sub>2</sub> or in dichloromethane (DC) solutions, using porphyrin concentrations in the range 0.1–0.5 mM.

**Resonance Raman Spectroscopy.** The resonance Raman spectra were recorded with two different experimental setups. Measurements were carried out either with backscattering or with a 90° scattering geometry to avoid the large spectral background caused by stray light reflected from the sample cell.

**Excimer Pumped Dye Laser System.** This setup was used when variable tuning of the excitation wavelengths was needed. An excimer laser (Lambda EMG53MSC) processing at 308 nm pumped a dye laser (Lambda FL2001) system. The output pulse energy of the latter was 0.5 mJ at a 200 Hz repetition rate and a pulse length of about 10 ns providing an average power of 100 mW. The linear polarized laser beam was filtered by two pinholes and focused by a cylindrical lens of 50 cm focal length onto the sample placed in a cylindrical rotating quartz cell. Rotation of the cell (50 Hz) prevented localized heating of the sample. The scattered light was collected and imaged onto the entrance slit of the spectrometer. A polarization analyzer between collimator and entrance slit was used to measure the Raman intensity of the two components parallel (||) and perpendicular (⊥) to the incident laser polarization. A polarization scrambler was placed in front of the entrance slit to avoid different transmissions of the spectrometer for the above polarization components.

The scattered light was dispersed by a Czerny-Turner monochromator (Spex 1877) equipped with a grating with 1200 grooves/mm. The geometrical slit *S* was adjusted to 50 μm. A preceding double monochromator was used as a filter to suppress stray light. The scattered light was detected by a CCD camera (Photometrics, CH 210) cooled with liquid nitrogen.

The spectral slit function was determined by recording the spectral lines of several pencil lamps (xenon, krypton, etc.).

**TABLE 1: C–C Stretch Force Constants (in mdyne/Å) Used in Molecular Mechanics and Force Field Calculations for All Porphyrins Investigated. Constants for nickel(II) Octaethylporphyrin (NiOEP) Listed for Comparison**

	NiOEP	NiOETPP	NiTEtP	NiMeP	NiTPP	NiTiPrP	NiTtBuP
C <sub>α</sub> –C <sub>β</sub>	5.495	5.429	5.316	5.302	5.316	5.429	5.269
C <sub>β</sub> –C <sub>β</sub>	7.482	7.209	7.874	7.940	7.973	7.841	7.641
C <sub>α</sub> –C <sub>m</sub>	8.179	7.236	7.522	7.615	7.681	7.449	7.279
C <sub>α</sub> –N	6.757	5.980	5.980	5.980	5.980	5.980	5.980

These lines are well approximated by Gaussians for the 50 μm slit width used in the experiments. The corresponding spectral width, defined by the full width at half-maximum (Fwhm), is 5.0 cm<sup>−1</sup> at 430 nm excitation (for a Stokes shift of 1000 cm<sup>−1</sup>). It has to be noted that the device-limited spectral resolution of the CCD array is about 1.5 cm<sup>−1</sup>, which is smaller than the spectral widths in our experiments.

The frequency calibration of the Raman spectra was carried out by using the intense CS<sub>2</sub> solvent line at 656.0 cm<sup>−1</sup> or the DC line at 703.2 cm<sup>−1</sup>. The dispersion of the spectrometer was earlier obtained using the spectra of the pencil lamps.<sup>18</sup> The wavelength dependence of the dispersion was accounted for in the calibration procedure. The maximum error of the observed line positions at different excitation wavelengths is 1.5 cm<sup>−1</sup>.

**CW Laser System.** Supplementary measurements with higher spectral resolution were carried out with CW excitation provided by either an argon ion laser (Spectra-Physics, Model 2020-05) or a krypton ion laser (Coherent, Innova 90 K). The plasma light of these lasers was suppressed using interference filters. Employing a cylindrical lens of 10 cm focal length, the linear polarized laser beam was focused onto the sample placed in the rotating cell. The scattered light was collected and imaged on the entrance slit of the spectrometer (Spex 1401) equipped with a CCD camera (Photometrics, SDS 9000) containing a 512 × 512 array chip (Site, TK 512 CB). The data were stored in a computer which also controls the motor of the spectrometer. Polarized Raman spectra were recorded using a polarization filter as analyzer (Spindler & Hoyer) and a scrambler placed in front of the entrance slit of the spectrometer.

The spectral slit functions were again determined by the spectral lines of pencil lamps (krypton, argon, etc), and can be described by convolution of a Gaussian and a boxcar function. The entrance slit was adjusted to *S* = 100 μm, thus providing a spectral width of about 2.7 cm<sup>−1</sup> or less. The frequency calibration was again performed using the most intense solvent line.

**Molecular Mechanics and Force Field Calculations.** The method employed for the geometry optimizations and the evaluation of normal modes has been described in a recent paper,<sup>15</sup> which besides others report a new force field for Ni(II) porphyrin (NiP) which contains significantly less force constants than that earlier reported by Li et al.<sup>19</sup> In general, the present study employs this force field with some minor changes. These mainly involve the C–C stretch parameters, which are significantly different (Table 1), since the C<sub>α</sub>–C<sub>β</sub> and the C<sub>β</sub>–C<sub>β</sub> force constants decrease with increasing degree of nonplanarity of the porphyrin macrocycle. The other stretch parameters show only minor variations, except for the large value of the C<sub>α</sub>–N force constant for NiOEP. We will refer to all these force constants in the Results and Discussion section.

The out-of-plane force constants of the macrocycle are in all cases identical with those obtained for NiP.<sup>15</sup> This force field consists of only five independent parameters, which are adjusted for NiP and kept fixed for all other porphyrins. We have checked our force constants in two ways. First, we compared our calculated frequencies of the A<sub>2u</sub> modes with those observed in



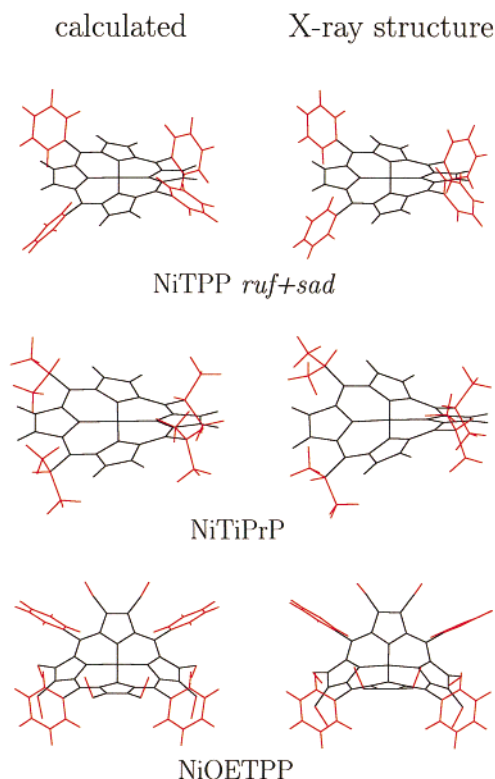


**Figure 2.** Comparison of the calculated and X-ray crystal structures of three strongly distorted porphyrins.

IR absorption spectra.<sup>20</sup> Second, we performed a normal-mode calculation for the related magnesium compound MgP by a density functional method using Becke 3LYP functional with 6-31 G\* and TZ2P basis sets. The DFT results were identical with those reported by Jarczycki et al.<sup>20</sup> Then we have compared the results of our empirical method with those obtained from the DFT approach. They turned out to be nearly identical with respect to both the eigenvectors and the frequencies, with the average frequency deviation being only 15 cm<sup>-1</sup>.

The unconstrained equilibrium bond lengths and the respective  $C_{\alpha}-N-C_{\alpha}$  angle used as parameters for the geometry optimization were adjusted to match the conformation of NiP known from an X-ray crystallographic study.<sup>21</sup> All other unconstrained angles for sp<sup>2</sup> hybridized atoms were set to 120°.

## Results and Discussion

The goal of the present study is the development of a spectroscopically determined molecular mechanics force field for porphyrins which self-consistently accounts for possible nonplanar distortions and the frequencies of vibrational modes as obtained by resonance Raman studies. In what follows we first discuss the results from molecular modeling of a series of meso-substituted porphyrins and compare them with available crystallographic data and molecular mechanics calculations by Jentzen et al., which was based on a Dreiding II force field and the conventional empirical force field for NiOEP. In a second step, the low-frequency spectra of the above porphyrins are introduced and the corresponding bands are assigned on the basis of normal-coordinate calculations performed for the minimal energy structure.

**Molecular Modeling.** Consistent with the results of Jentzen et al.,<sup>9</sup> our calculations show that all meso-tetrasubstituted porphyrins exhibit ruffled conformations. The structures obtained for NiTPP and NiTiPrP are shown in Figure 2 and are compared with the corresponding conformations known from

X-ray crystallographic studies. The ruffling distortion, which is of type B<sub>1u</sub>, yields a twist of the pyrrole planes with respect to each other. Therefore, the degree of ruffling can be quantified by the angle between the planes of two opposite pyrroles which is identical for the two pyrrole pairs. A similar angle designated as the *ruf* angle has been introduced earlier.<sup>4,9</sup> If an additional type of distortion is present, like the small degree of saddling observed for NiTPP, more care must be taken when defining the *ruf* angle. As is obvious for NiOETPP in Figure 2, the strong saddling also causes a rotation of the pyrrole planes, which involves a tilt rather than a torsion around the N–Ni–N bond. Therefore, pyrrole tilting needs to be distinguished from torsion which led us to follow ref 4 in introducing the *sad* angle N–Ni–N.

Some important structural parameters that emerged from our molecular mechanics calculations are listed in Table 2, together with the corresponding values obtained from X-ray crystallographic studies for comparison. The *ruf* angle increases in the order NiTetP, NiTMeP, NiTPP, NiTiPrP, and NiTtBuP. This is in agreement with the observations of Jentzen et al.,<sup>9</sup> except for NiTPP where a planar conformation was suggested by their molecular mechanics calculations. Later studies<sup>12,13</sup> indicated a ruffled conformation of NiTPP in solution and also in the crystallized form.<sup>11</sup> In solution, (quasi)planar and ruffled conformers of NiTPP coexist with a preference for the ruffled conformation.<sup>13</sup> Later molecular mechanics calculations<sup>12</sup> predicted three different conformations of NiTPP, a planar structure with *D*<sub>4h</sub> symmetry, a slightly saddled structure, and a significantly ruffled structure. Our results shown in Table 2, however, reveal only one stable conformation. Depending on what is assumed for the force constant of phenyl torsion with respect to the porphyrin plane, this conformation is either planar or slightly saddled. We have chosen a value for this force constant which reproduces the known saddled conformation of NiOETPP (see Figure 2), and based on this approach we then found that the phenyls with parallel orientation slightly stabilize the molecules'  $\pi$ -system by 20 kJ/mol compared to the perpendicular conformation. Taking all intramolecular interactions into account, the saddled conformation of NiTPP is calculated to be more stable than the planar one and this is the one listed in Table 2.

This table lists an additionally calculated conformation, namely *ruf* + *sad*, which is also shown in Figure 2. This structure does not correspond to a minimum in the potential used for our calculation. It was obtained by performing the geometry optimization procedure in a special way. We used the conformation of crystallized NiTPP as the starting point in the configurational space. A restriction was then imposed onto the optimization process in that we prevented the structure from varying along the normal coordinates of the two ruffling modes exhibiting the lowest frequencies, i.e., the phenyl up–down translation at 39 cm<sup>-1</sup> and the macrocycle mode  $\gamma_{14}$  at 88 cm<sup>-1</sup>. Interestingly, the saddling contribution is predicted nearly correctly, although the structure was allowed to vary along all saddling coordinates. The saddling distortion is obviously imposed by the orientation of the phenyl rings which are not perpendicular to the porphyrin plane. This is valid for both the predicted and the X-ray observed structure, although the angle is closer to 90° in the crystal conformation. Later, we will refer to the reasons why the *ruf* + *sad* conformation is unstable and 15.7 kJ/mol higher in energy than the lowest energy saddle conformation in our calculation.

The general agreement between the predicted and X-ray observed structures in Table 2 is not fully satisfying, but the

**TABLE 2: Selected Structural Parameters Obtained from Calculated Lowest Energy Conformations and X-ray Crystal Structures<sup>a</sup>**

	core size (deg)	ruf angle (deg)	sad angle (deg)	C <sub>α</sub> NC <sub>α</sub> angle (deg)	C <sub>α</sub> C <sub>β</sub> bond (Å)	C <sub>β</sub> C <sub>β</sub> bond (Å)	C <sub>α</sub> C <sub>m</sub> bond (Å)	C <sub>α</sub> N bond (Å)	C <sub>α</sub> N torsion (deg)
NiTEtP									
ruf αβαβ	1.962	13.3	0.0	106.1	1.435	1.339	1.369	1.389	4.2
NiTMeP									
ruf αβαβ	1.956	17.1	0.0	106.1	1.435	1.340	1.369	1.388	7.1
X-ray <sup>b</sup>	1.938	17.3	13.9	105.2	1.446	1.340	1.387	1.382	6.9
X-ray <sup>c</sup>	1.934	17.1	15.1	104.8	1.436	1.353	1.391	1.381	6.3
X-ray <sup>d</sup>	1.950	3.5	2.9	104.7	1.436	1.335	1.380	1.388	4.1
X-ray <sup>e</sup>	1.958	1.0	0.3	104.6	1.443	1.344	1.384	1.384	0.6
NiTMeP (+ - + -)									
sad	1.959	0.1	8.2	105.8	1.435	1.340	1.367	1.387	3.3
ruf + sad <sup>f</sup>	1.941	23.3	7.4	106.2	1.434	1.341	1.396	1.386	8.3
X-ray <sup>g</sup>	1.929	27.9	5.3	105.0	1.435	1.357	1.384	1.380	8.7
NiTiPrP									
ruf	1.949	24.2	0.9	106.5	1.434	1.341	1.373	1.392	9.9
X-ray <sup>h</sup>	1.896	43.8	4.4	106.1	1.432	1.341	1.392	1.384	14.0
NiTTBuP									
ruf αβαβ	1.908	42.7	0.0	107.8	1.432	1.345	1.381	1.391	21.3
NiOETPP									
sad	1.941	0.0	39.8	105.9	1.438	1.350	1.384	1.384	14.1
X-ray <sup>i</sup>	1.905	2.3	45.1	105.9	1.452	1.361	1.395	1.381	15.0

<sup>a</sup> α and β indicate to an up and down orientation of the alkyl substituents. + and - mean a clockwise and counterclockwise rotation of the phenyl groups of NiTPP and refer also to the orientation of the isopropyl substituents. <sup>b</sup> Partially oxydized NiTMeP iodide crystal structure from ref 28. <sup>c</sup> bis(NiTMeP) hexafluorophosphate, ref 29. <sup>d</sup> NiTMeP 7,7,8,8-tetracyanoquinodimethane, ref 30. <sup>e</sup> bis(NiTMeP) perrhenate, ref 31. <sup>f</sup> This conformation is not stable in our harmonic force field approach. <sup>g</sup> NiTPP crystal, ref 11. <sup>h</sup> NiTiPrP crystal, ref 32. <sup>i</sup> NiOETPP methanol solvate at 200 K, ref 14c.

trends for the relative changes of the parameters are calculated correctly. The core size is generally overestimated, with the deviation being especially large for the highly distorted porphyrins for which the degree of ruffling is also not correctly predicted. Most of the C-C bond lengths are underestimated, while C<sub>α</sub>-N is slightly too large in the calculated structures. On the other hand, the calculations reveal the correct correlation between the core size and the degree of ruffling, i.e., the core size decreases with increasing nonplanarity. The dependence of the C-C bond lengths from the degree of ruffling is also satisfactorily predicted, i.e., C<sub>α</sub>-C<sub>m</sub> and C<sub>β</sub>-C<sub>β</sub> increase for nonplanar porphyrins, while C<sub>α</sub>-C<sub>β</sub> and C<sub>α</sub>-N behave indifferently. In general, deviation between the structure in the crystal and solution may exist due to the absence of packing forces in the latter.

It is interesting in this context that the bond length changes are consistent with the systematic behavior of the corresponding stretch force constants (cf. Tables 1 and 2). It is known<sup>4,19</sup> that the normal modes with major contributions of C<sub>α</sub>-C<sub>m</sub> and C<sub>β</sub>-C<sub>β</sub> shift down with increasing degree of nonplanarity, while other C-C stretch modes show a less pronounced or even no correlation. As expected, the C<sub>α</sub>-C<sub>m</sub> and C<sub>β</sub>-C<sub>β</sub> stretch force constants decrease for the nonplanar porphyrins, as listed in Table 1. As has been reported earlier,<sup>19</sup> the stretch force constants *f* are proportional to the inverse of the third power of the bond length *r*, i.e.,  $f \approx r^{-3}$ . The functional dependence of the frequency is therefore  $\nu \approx r^{-3/2}$ . Thus, the calculated change of the C<sub>α</sub>-C<sub>m</sub> bond length of 0.012 Å for NiTTBuP compared with NiTEtP should result in a frequency shift of about 20 cm<sup>-1</sup> for ν<sub>10</sub> and ν<sub>19</sub> which are nearly pure C<sub>α</sub>-C<sub>m</sub> stretching modes.<sup>19</sup> ν<sub>19</sub> is observed at 1564 cm<sup>-1</sup> for NiTEtP<sup>19</sup> and at 1515 cm<sup>-1</sup> for NiTTBuP (inferred from our Q<sub>v</sub>-excited Raman spectra, data not shown). The observed shift of 49 cm<sup>-1</sup> is larger, but in the same order of magnitude as the predicted shift. Unfortunately, the frequency position of ν<sub>10</sub> is not available for NiTTBuP. For the C<sub>β</sub>-C<sub>β</sub> modes, a much smaller frequency shift is expected. The most suitable marker mode to check this is ν<sub>11</sub>. Its

assignment, however, is not very reliable for NiTTBuP because of the lack of Q<sub>0</sub>-excited Raman spectra, in which B<sub>1g</sub> type modes are generally most intense. According to Jentzen et al.,<sup>9</sup> the shift is in the same order as for the C<sub>α</sub>-C<sub>m</sub> stretching modes, namely 37 cm<sup>-1</sup>. This would contradict our prediction, but more reliable data are necessary for a final proof.

Another geometric parameter probably important for the frequencies of marker modes is the C<sub>α</sub>-C<sub>m</sub> torsion<sup>9</sup> which is also listed in Table 2. It is defined as the angle between the p<sub>z</sub> orbitals of two neighboring C<sub>α</sub>,C<sub>m</sub> atoms. We assume these orbitals to be perpendicular to the plane defined by the respective neighboring atoms, i.e., NC<sub>α</sub>C<sub>m</sub> and HC<sub>β</sub>C<sub>α</sub>. The torsion angle is zero for planar porphyrins and increases with the degree of ruffling. According to Jentzen et al.,<sup>9</sup> this torsion is not affected by saddling. These authors therefore suggested that the marker mode frequencies may be less sensitive to saddling than to ruffling, and they hoped to be able to distinguish between these different types of nonplanar distortions. However, recent NMR studies on the ring current of nonplanar porphyrins suggest that nonplanar distortions affect the C<sub>m</sub>-C<sub>α</sub> π-electron conjugation and thus the above torsional angle.<sup>22</sup> Our results also suggest that the torsional angle is changed by saddling. It is obvious from Table 2 that C<sub>α</sub>-C<sub>m</sub> torsion is effected by saddling in the same order of magnitude as by ruffling. Furthermore, Piffat et al.<sup>17</sup> provided evidence that the core size markers are sensitive to saddling and ruffling in that they showed that the C<sub>α</sub>-C<sub>m</sub> stretching mode frequencies of NiOETPP depend on saddling. The frequency of ν<sub>19</sub>, for instance, is overestimated by more than 70 cm<sup>-1</sup>, if the corresponding force constants of the planar porphyrins are used. Thus, we doubt that the type of distortion can be identified by investigating only the marker mode frequencies.

As stated above, the degree of ruffling is underestimated in our molecular mechanics results for highly nonplanar porphyrins. This becomes obvious not only by comparison of the calculated and observed structural parameters but also in view of the results of Jentzen et al.,<sup>9</sup> who have investigated some

**TABLE 3: Observed and Calculated Frequencies ( $\text{cm}^{-1}$ ) of the Franck–Condon Active Low-Frequency ( $<1000 \text{ cm}^{-1}$ ) Modes (Type  $B_{1u}$  and  $A_{1g}$ ) for the Meso-Substituted Porphyrins<sup>a</sup>**

	$\gamma_{13}$	$\gamma_{11}$	$\gamma_{12}$	$\gamma_{10}$	$\nu_6$	$\nu'_7$	$\nu_7$	$\nu_8$
NiTEtP								
obs	891	740	495	316	983		544	379
calc	865	702	503	301	922		566	374
NiTMeP								
obs	890		491		995		522	376
(0)			(1)		(~20)		(>10)	(6)
calc	861	677	487	211	943		508	367
(0)		(16)	(3)	(14)	(27)		(36)	(7)
NiTPP								
obs <sup>b</sup>	904	737	552	333	1005	889	640	391/401
(0,0,-,0)		(1,5,-,-)	(0,9,25,12)	(1,0,11,6)	(23,0,1,7)	(3,13,-2,-)	(1,0,0,25)	(3,0,9,2)
calc								
sad	875	701	523	298	1016	856	650	398
ruf + sad	881	710	527	298	1016	857	649	406
(0,2,109,0)		(0,7,57,4)	(2,6,42,3)	(0,0,8,8)	(21,4,5,8)	(1,8,1,-7)	(0,3,1,14)	(3,0,8,1)
NiTiPrP								
obs	893	742	544	417	945	—	590	359
calc	893	766	576	433	927	812	607	353

<sup>a</sup>  $\nu'_7$  denotes a substituent mode with macrocycle contributions to the eigenvector similar to  $\nu_7$ . Corresponding isotopic shifts for each mode are listed in parentheses, namely ( $^{15}\text{N}_4$ ,  $^{13}\text{C}_4$ ,  $d_8$ ,  $d_{20}$ ) for NiTPP and ( $d_{12}$ ) for NiTMeP. A positive sign means that the mode shifts to lower wavenumbers upon isotopic substitution. <sup>b</sup> The isotopic shifts were obtained from ref 24.

more meso-substituted porphyrins. In their study, the degree of ruffling is also underestimated, even though it is generally larger than that obtained in our study. The underestimation of ruffling probably reflects a breakdown of the harmonic approximation for the ruffling potential of strongly distorted systems. Such an anharmonicity may result from the weakening of the  $\pi$ -electronic bonds as it occurs in a ruffled conformation. An anharmonic approach for this potential should therefore yield better results for the predicted structures. This notion is corroborated by results from a recent analysis of the temperature dependend absorption spectra of various metallo-octaethylporphyrins, which are indicative of a partially strong, metal-dependent anharmonicity of out-of-plane modes.<sup>23</sup>

Our harmonic approach for the ruffling potential is probably also the reason for the instability of the NiTPP conformation in our molecular mechanics calculation. Its energy is predicted to be only 15.7 kJ/mol higher than that of the most stable quasiplanar sad conformation. This value must be compared with the cost of energy for inducing macrocycle ruffling as obtained for NiTPP, namely 28 kJ/mol.<sup>8</sup> If the latter were overestimated by the harmonic approximation by e.g. 18 kJ/mol, the ruf + sad conformation would be slightly more stable than the quasiplanar one, as is observed in a Raman study of NiTPP in  $\text{CS}_2$ .<sup>21</sup> Therefore, our calculations do not necessarily contradict the observed enthalpy differences between the NiTPP conformers.

Table 3 further reveals that the frequency of  $\nu_8$  is predicted to be higher for the ruf + sad than for the planar conformation. This is in line with two studies on NiTPP in  $\text{CS}_2$ <sup>12,13</sup> showing that  $\nu_8$  is composed of two subbands separated by  $10 \text{ cm}^{-1}$ , with the high-frequency subband assignable to the ruffled conformer. Our normal-mode calculation also predicts a conformational dependence of the frequencies of some other modes, i.e.,  $\gamma_{13}$ ,  $\gamma_{11}$ ,  $\gamma_{12}$ . This finding explains the relatively broad band shapes of the corresponding Raman bands (Figure 3).

A further point of interest is the structural variety of the NiTMeP conformations found in the crystal structures (cf. Table 2). The porphyrin conformation is obviously very flexible to accommodate changes in its environment. Two of the structures exhibit a ruffling very close to the predicted one. Additionally, they exhibit a significant degree of saddling. The two other

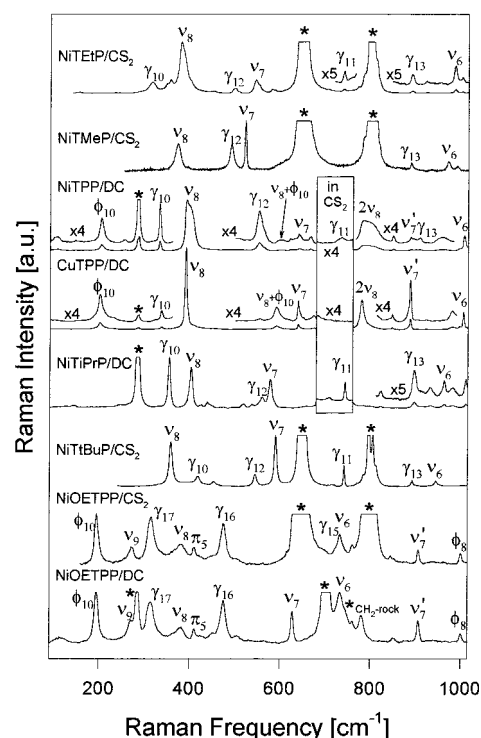


**Figure 3.** Raman spectra taken from Soret excitation and band assignments for all porphyrins investigated. Lines arising from the solvent, namely  $\text{CS}_2$  or dichloromethane (DC), are marked by a \*. Only spectra measured polarized parallel to the incident polarization are shown. Because DC has solvent bands in the region between 680 and  $760 \text{ cm}^{-1}$ , spectra of NiTPP, CuTPP, and NiTiPrP in  $\text{CS}_2$  are shown instead of those measured with DC for this spectral range (inset). Laser excitation is at  $406.7 \text{ nm}$  except for NiTEtP ( $441.6 \text{ nm}$ ), NiTiBuP ( $472.7 \text{ nm}$ ), and NiOETPP ( $445 \text{ nm}$  for  $\text{CS}_2$  and  $435 \text{ nm}$  for DC). The spectral sections shown in the inset are measured at  $425 \text{ nm}$  for NiTPP, at  $435 \text{ nm}$  for CuTPP, and at  $457.9 \text{ nm}$  for NiTiPrP.

structures are nearly planar. As has been argued,<sup>9</sup> the existence of planar forms is not surprising because they are predicted to be only 3.5 kJ/mol above the most stable ruf conformation. Porphyrins with more bulky substituents such as NiTiBuP and NiOETPP can be expected to be less flexible. Indeed, X-ray



investigations of their crystal structure show only one conformation for each of these molecules. Furthermore, the core size marker bands of these porphyrins in organic solution can all be fit by a single band, which also indicates that only one conformation is present. This is likely due to the strong steric interactions between the substituents.

**Raman Spectra and Assignments.** We have measured polarized Raman spectra with Soret resonance excitation for all porphyrins investigated. In what follows we confine ourselves on discussing the low-frequency regions of these spectra in which one expects to find Raman bands arising from out-of-plane modes. By their identification, we are able to unambiguously obtain the modes of out-of-plane distortions of the corresponding porphyrin macrocycles.

The low-frequency regions of some spectra ( $<1000\text{ cm}^{-1}$ ) recorded with parallel polarization are shown in Figure 3. These spectra were measured in the polarization parallel to the incident one. They mostly display Raman bands the intensity of which mainly results from Franck–Condon type coupling.<sup>3</sup> The intense polarized bands appearing in these spectra were assigned by virtue of our normal mode calculations. Some of the bands arise from  $A_{1g}$  modes, which are generally Franck–Condon active for all porphyrins. Some other bands, however, have to be assigned to out-of-plane modes, which are not Raman allowed in  $D_{4h}$  symmetry. For the meso-substituted porphyrins, which are expected to be ruffled, all  $B_{1u}$  modes within the observed frequency range were found to be Raman active. These are the modes  $\gamma_{10}$ ,  $\gamma_{11}$ ,  $\gamma_{12}$ , and  $\gamma_{13}$ . We have calculated the eigenvectors and frequencies of these modes for all meso-substituted porphyrins and also for related model systems NiTCP\* (nickel meso-tetracarboxyporphyrin, \* labels it as an artificial model system), in which all substituents are replaced by a point mass of 12 u (i.e., the mass of a carbon atom). The eigenvectors of the latter are depicted in Figure 4. It turned out that corresponding modes with very similar eigenvectors and frequencies are obtainable for the fully substituted porphyrins and the respective model systems. This suggests that the simple model system provides a sound basis for calculating macrocycle modes accurately. Moreover, the calculations for the model system and related fully substituted porphyrins allow to distinguish between macrocycle and substituent modes.

Figure 4 also shows the  $B_{1u}$  type modes for another model system, namely NiOEP with its ethyl substituents substituted by carbon atoms. It is designated as NiOCP\* (nickel(II) octacarboxyporphyrin). This particular artificial system is of interest because NiOEP serves as a reference system for the numbering scheme of the macrocycle modes. Therefore, in order to obtain a reasonable mode designation for the meso-substituted compounds, we now compare the calculated macrocycle modes of the model systems NiOCP\* and NiTCP\* to identify pairs with most similar patterns.

$\gamma_{10}$  of NiOCP\* ( $836\text{ cm}^{-1}$  calculated) is mainly a  $C_m$ –H out-of-plane wagging mode. It can easily be correlated with the  $C_m$ – $C_{\text{subst}}$  out-of-plane wagging of NiTCP\* ( $250\text{ cm}^{-1}$ ), because, apart from  $\gamma_{14}$ , it is the only mode with  $C_m$ –H (or  $C_m$ – $C_{\text{subst}}$ ) wagging contributions (cf. Table 3). A similar argumentation holds for  $\gamma_{13}$ , which is  $C_\beta$ –H out-of-plane wagging mode for NiTCP\* ( $856\text{ cm}^{-1}$ ) and  $C_\beta$ – $C_{\text{subst}}$  for NiOCP\* ( $202\text{ cm}^{-1}$ ). The two remaining modes are more difficult to attribute.  $\gamma_{12}$  and  $\gamma_{14}$  of NiOCP\* involve pyrrole rotation combined in-phase and out-of-phase with the up and down motions of the methin carbons, respectively. For NiTCP\*, the mode exhibiting a frequency of  $503\text{ cm}^{-1}$  closely matches this description.  $\gamma_{11}$  has significant contributions of pyrrole folding, a feature which

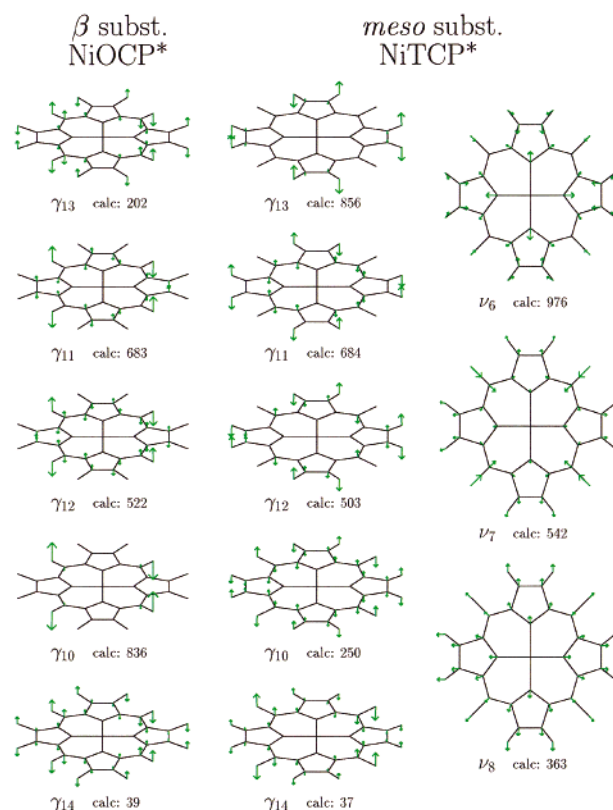


**Figure 4.** Comparison of the cartesian atomic displacements for the  $B_{1u}$  type modes of  $\beta$ - and meso-substituted porphyrins, for which the substituents are replaced by a point mass of 12 u. Additionally, the low-frequency modes of type  $A_{1g}$  are shown for the meso-substituted system.

mostly appears in the eigenvector of the mode at  $684\text{ cm}^{-1}$ , although it looks somewhat different because the hydrogens are strongly involved in this vibration.

Further support for our assignment of the ruffling modes of NiTPP is provided by comparison with the Raman spectra of NiTPP and CuTPP in Figure 3. Because CuTPP is (quasi)planar in solution,<sup>18</sup> the  $B_{1u}$  modes are expected to disappear in the spectra of this compound. This is indeed the case for  $\gamma_{11}$ ,  $\gamma_{12}$ , and  $\gamma_{13}$ .  $\gamma_{10}$ , however, is still present for CuTPP, though with much smaller intensity. This can be rationalized, however, because this mode shows significant contributions from the phenyl groups, which are unlikely to be perpendicularly oriented with respect to the porphyrin plane, so that it also exhibits some in-plane contributions. Another possible explanation is that CuTPP is slightly ruffled in solution. This interpretation is consistent with the appearance of a weak line at the frequency position of  $\gamma_{12}$  in the spectrum of CuTPP.

The calculated and experimentally observed frequencies of the  $A_{1g}$  and  $B_{1u}$  type modes for the meso-substituted porphyrins with frequencies between 100 and  $1000\text{ cm}^{-1}$  are listed in Table 3. Two of the  $A_{1g}$  modes exhibit a mode pattern typical for  $\nu_7$ , i.e.,  $C_\alpha C_m C_\alpha$  bending and stretching of the pyrroles. For NiTPP (and also for NiOETPP (cf. Figure 6)), they give rise to Raman bands at  $889$  ( $905$ ) and  $640$  ( $627$ )  $\text{cm}^{-1}$ . The corresponding eigenvectors exhibit significant contributions from both macrocycle and substituents vibrations. The pattern of the  $640$  ( $627$ )  $\text{cm}^{-1}$  mode contains strong contributions from phenyl vibrations, which are similar to  $\nu_6$  of benzene in the Wilson notation. This led Li et al.<sup>19</sup> to describe it as a substituent mode designated as  $\phi_9$ . Consequently, these authors identified the other mode observed at  $889$  ( $905$ )  $\text{cm}^{-1}$  with the macrocycle mode  $\nu_7$ . This interpretation, however, is not consistent with the observation

that a mode assignable to  $\nu_7$  does not appear in the 800–900  $\text{cm}^{-1}$  Raman spectra of the other meso-substituents nor in the calculated vibrational spectrum of NiTCP\*. This clearly suggests that the 889 (905)  $\text{cm}^{-1}$  vibration is assignable to a (phenyl ring) substituent mode which we now designate as  $\nu'_7$  because of its similarity with this macrocycle vibration, whereas the 640 (627)  $\text{cm}^{-1}$  vibration is assigned to  $\nu_7$ .

Further evidence for our assignment is provided by comparing of the calculated frequency shifts for several isotopic derivatives with the observed ones reported elsewhere.<sup>24</sup> For NiTMeP, Table 3 lists the shifts for the  $d_{12}$  derivative, in which all hydrogens of the methyl groups are replaced by deuterium. Most of the calculated values are in good agreement with the calculated ones. The  $\nu_7$  now appears in a spectral region which is already crowded by other bands, so that its shift can only be crudely estimated. For NiTPP, a large body of data for isotopic derivatives are available. The  $^{13}\text{C}_4$  derivative has all its meso carbons substituted,  $d_8$  labels a compound in which the hydrogens at the  $\beta$  positions are deuterated, while all phenyl hydrogens are exchanged against deuterium in the  $d_{20}$  form. In general, the obtained correspondence between observed and calculated frequencies support our assignment, even though some significant deviations cannot be neglected. These, however, are comparable or even smaller than those obtained in other studies.<sup>17,19,25</sup> They are likely caused by slight errors in calculating the hydrogen contribution to the modes eigenvectors.

Some of our assignments deviate from those proposed by Li et al.<sup>19,25</sup> First, they attributed the band at 890  $\text{cm}^{-1}$  to  $\nu_7$  for NiTEt and NiTMeP. For the latter, however, this mode is expected to shift upon  $d_{12}$  substitution (see Table 3). The spectra of Li et al. clearly show that such a shift is not present for this Raman line. Therefore, the assignment of this band to  $\gamma_{13}$  is more reasonable. Second, there are also some deviations for NiTPP. The Raman line at 333  $\text{cm}^{-1}$  was assigned to  $\gamma_2$ , but this is at odds with its depolarization ratio (DPR) being close to 0.125. In the presence of  $B_{1u}$  distortions, an  $A_{1u}$  type mode as  $\gamma_2$  should exhibit a DPR of 0.75. Because the DPR of depolarized bands is not dispersive for NiTPP,<sup>13</sup>  $\gamma_2$  cannot yield a band of DPR 0.125 in the Raman spectra. Third, as already mentioned above, the band which we have assigned to  $\nu_7$ , was attributed to  $\pi_9$  by Li et al.

We also found a reasonable assignment for the band near 600  $\text{cm}^{-1}$ , which is present in the spectra of both tetraphenylporphyrins investigated. For the crystal form of NiTPP (3,1,-11,9) its isotopic shift pattern<sup>20</sup> is very close to the sum of the shift patterns (0,0,0,6) and (4,1,11,2) of  $\pi_{10}$  and  $\nu_8$ , respectively. This band, which is at 602  $\text{cm}^{-1}$  for NiTPP, obviously arises from the combination of these two modes, the band positions of which are listed in Table 3. Another interesting band appearing at 790  $\text{cm}^{-1}$  is assigned to  $2\nu_8$ . It shows a subband structure which is consistent with that of  $\nu_8$ . The subband positions are at 782 and 801  $\text{cm}^{-1}$ , which are both twice the subband position of  $\nu_8$ , and the intensity ratio of the subbands is identical in the limit of accuracy. These findings provide strongly the notion that the subbands arise from coexisting conformers.<sup>12,13</sup> As expected,  $2\nu_8$  appears as a single line in the spectrum of CuTPP.

For NiOETPP, our normal-mode analysis is essentially consistent with that of Piffat et al.<sup>17</sup> However, in contrast to their strategy, we have calculated the modes by taking into account the saddled conformation of this porphyrin, as shown in Figure 2. All atoms of NiOETPP are included in our analysis, except the hydrogens of the ethyl groups. Therefore, our calculation reproduces all normal modes with sufficient accuracy

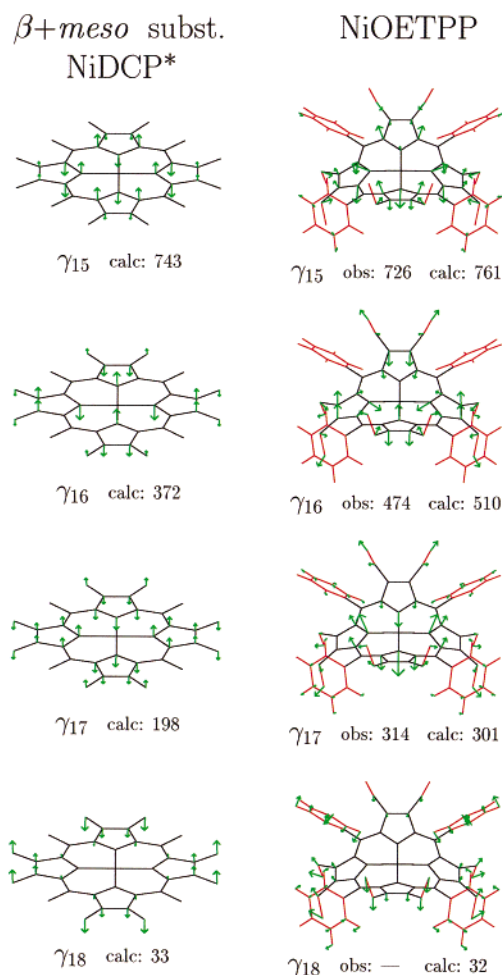


**Figure 5.** Cartesian atomic displacements for the  $B_{2u}$  pseudotype modes of NiOETPP and for a simple model, in which the substituents are replaced by 12 u point masses.

except the ethyl modes. The latter are reported in ref 17 and do not significantly differ from those for NiOEP. The  $B_{2u}$  modes obtained by our analysis are shown in Figure 5. To avoid confusion, we have also depicted the respective modes of the corresponding simplified model system with 12 u masses. Close inspection of the mode eigenvectors shows that the modes are similar for the simple model system and for the saddled porphyrin. However, it can also be inferred from the figure that the out-of-plane distortion causes significant deviations of the Cartesian displacement vectors. Some of these vectors do not point perpendicular to the porphyrin plane, but have in-plane components. This becomes even clearer by inspection of Figure 6, in which three of the saddling modes are shown from the top view. From this perspective these modes look like in-plane modes of type  $A_{1g}$ . Some of the latter are also depicted in the figure. Because in-plane and out-of-plane contributions mix in the eigenvectors, the  $A_{1g}$  modes are not strictly in-plane. This mixing is especially strong (nearly 50:50) for the modes  $\gamma_{15}$  and  $\nu_6$ , and the designation of these modes is therefore more or less arbitrary. A similar situation is also present for the modes  $\gamma_{10}$  and  $\nu_8$  of NiTiPrP and NiTtBuP. Because the in- and out-of-plane mixing is nearly 50:50 for NiTiPrP, the corresponding Raman modes exhibit similar intensities.  $\gamma_{12}$  and  $\nu_7$  are also hard to distinguish for some of the meso-substituted porphyrins. These examples show that in- and out-of-plane mixing becomes in particular effective, when the respective in- and out-of-plane modes are close together in frequency.



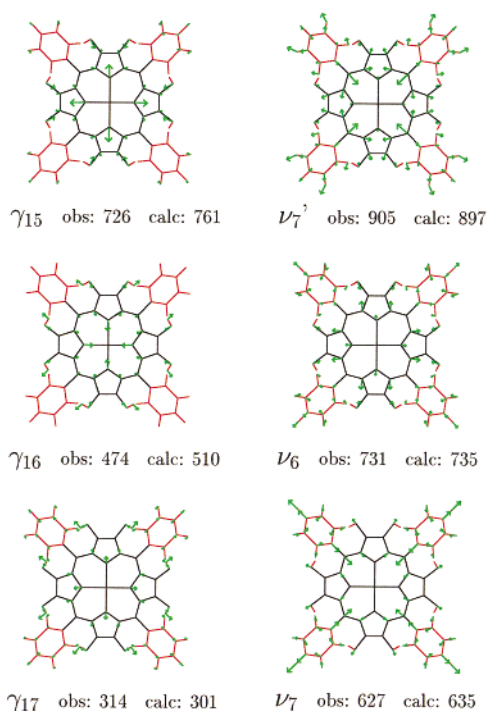


**Figure 6.** (Left column) Three of the  $B_{2u}$  pseudotype modes in top view to illustrate the strong in-plane contributions to these modes' eigenvectors. (Right column) Modes of pseudotype  $A_{1g}$  for which our designation is different from refs 16 and 17.

The mode assignments for the  $A_{1g}$  and  $B_{2u}$  macrocycle modes of NiOETPP in the frequency region between 100 and 1000  $\text{cm}^{-1}$  are listed in Table 4 together with the isotopic shifts for three different derivatives. The  $^{13}\text{C}_4$  and the  $\text{d}_{20}$  species are comparable with those of NiTPP. As can be seen from Table 3, the observed and calculated shifts are in agreement within the expected limit of accuracy. Our assignments and designations are not identical for all modes with that of Piffat et al.<sup>17</sup> These authors have considered the  $\gamma_{16}$  as a substituent mode. Consequently, they designated 314  $\text{cm}^{-1}$  mode as  $\gamma_{16}$ . The mode nomenclature is also different for the  $A_{1g}$  type vibrations  $\nu_6$  and  $\nu_7$ . Similarly to NiTPP, a substituent mode  $\nu_7$  exists for NiOETPP, which has a mode pattern comparable with  $\nu_7$ . Lines resulting from these three modes appear in the Raman spectra. Piffat et al. have attributed the highest frequency line, which we have assigned as  $\nu_7$ , to  $\nu_6$ . Further, they assigned the line at 731  $\text{cm}^{-1}$  to  $\nu_7$ , while the remaining lowest frequency mode was attributed to  $\nu_{33}$ . The latter assignment contradicts the value found for the DPR, i.e., 0.125. For  $\nu_{33}$  a DPR of 0.75 would be expected, and this is even valid in view of the DPR dispersion found by Schweitzer-Stenner et al.,<sup>3c</sup> because only  $A_{1g}$  and  $A_{2g}$  modes are dispersive. Furthermore, our assignment of  $\nu_7$  and  $\nu_6$  is also more convincing because  $\nu_6$  is generally the mode exhibiting a comparably large shift upon  $^{15}\text{N}_4$  isotopic substitu-

tion.<sup>19,25</sup> This requirement is not met by the assignment suggested by Piffat et al.<sup>17</sup> The mode assignment of Stichternath et al.<sup>16</sup> is also not satisfying in this respect, because they also attributed the line at 731  $\text{cm}^{-1}$  to  $\nu_7$ . According to these authors, the  $\nu_6$  appears as a relatively weak line at 849  $\text{cm}^{-1}$ . Our normal-mode calculations suggest instead, that this line does not arise from a fundamental macrocycle mode.

There is also a peculiarity with respect to the assignment of the line at 999  $\text{cm}^{-1}$ . This line was surprisingly attributed to  $\phi_7$  by Piffat et al.,<sup>17</sup> although these authors showed that the observed shift of 42  $\text{cm}^{-1}$  upon  $\text{d}_{20}$  substitution is by far too small for this mode, which is expected to be in the order of 220  $\text{cm}^{-1}$ . We agree with Stichternath et al.<sup>16</sup> in that this Raman line is assigned to  $\phi_8$ , and we have calculated a shift of 38  $\text{cm}^{-1}$  for this mode.

An interesting feature of the Raman spectra of NiOETPP is the appearance of the out-of-plane phenyl mode  $\pi_5$  in the Raman spectra as a polarized line. This provides evidence that the phenyl groups are not perpendicular to the porphyrin plane. In a 90° geometry  $\pi_5$  would solely contain contributions of  $B_{1g}$  and  $A_{2u}$  symmetry type with respect to the group  $D_{4h}$ . This would yield a DPR of 0.75. When the phenyls are rotated out of the perpendicular orientation, however, as is the case for both the crystal and the calculated conformation,  $\pi_5$  no longer reduces the symmetry of the molecule and therefore becomes Franck–Condon active. Its DPR is typical for a polarized band and is about 0.125. Thus, the phenyl groups are also not perpendicularly orientated for the conformation in solution.

## Conclusions

By means of our molecular mechanics and normal-mode calculation method we were able to predict the conformations of the porphyrins investigated and we have obtained the normal modes of these nonplanar compounds. We have assigned all prominent polarized bands in the Raman spectra between 100 and 1000  $\text{cm}^{-1}$ . The modes' frequencies and isotopic shift patterns are in satisfactory agreement with the observed ones.

With this information at hand we are now able to make precise statements about the conformations of these porphyrins in noncoordinative solution. All meso-substituted porphyrins exhibit ruffled  $B_{1u}$  distorted conformations which are identical or similar to the respective predicted ones or those observed in the crystal structures. It can also be shown that saddling is low or even not present for these porphyrins, because no Raman lines appear at the positions predicted for the saddling modes  $\gamma_{17}$ ,  $\gamma_{15}$ , and  $\gamma_{16}$ , which are at  $\approx 800$ , 700, and 270  $\text{cm}^{-1}$ , respectively.  $\gamma_{18}$  is too low in frequency to be observed in our Raman spectra. Therefore, NiTMeP, NiTEtP, NiTiPrP, and NiTtBuP are ruffled and not saddled in solution. For the tetraphenylporphyrins, a small polarized Raman line slightly above  $\pi_{10}$  appears in the spectra which may be attributed to  $\gamma_{16}$ , an assignment which is in line with recent evidence for a

**TABLE 4: Observed and Calculated Frequencies of the Franck–Condon Active Low-Frequency Modes (Type  $B_{2u}$  and  $A_{1g}$ ) for NiOETPP<sup>a</sup>**

	$\gamma_{15}$	$\gamma_{16}$	$\gamma_{17}$	$\nu_7'$	$\nu_6$	$\nu_7$	$\nu_8$	$\nu_9$
NiOETPP								
obs <sup>b</sup>	726	474	314	905	731	627	363/379	267
	(−,0,−4)	(2,0,0)	(0,0,0)	(0,12,6)	(6,0,9)	(2,4,19)	(0,0,0/4)	(2,0,0)
calc	761	510	301	897	735	635	329	290
	(6,0,0)	(4,1,1)	(4,0,1)	(0,10,4)	(6,1,10)	(1,4,11)	(1,0,0)	(2,0,1)

<sup>a</sup>  $\nu_7'$  denotes a substituent mode with macrocycle contributions to the eigenvector similar to  $\nu_7$ . Corresponding isotopic shifts are listed in parentheses, according to the syntax ( $^{15}\text{N}_4$ ,  $^{13}\text{C}_4$ ,  $\text{d}_{20}$ ). A positive sign means that the mode shifts to lower wavenumbers upon isotopic substitution.

<sup>b</sup> The isotopic shifts were obtained from ref 17.

small but significant saddling distortion of NiTPP in noncoordinative solution.<sup>13</sup>

The degree of ruffling of the porphyrin macrocycle increases as the steric bulk of the substituents gets larger. The former is evident in the increase of the Raman intensities corresponding to B<sub>1u</sub> modes. Especially, the  $\gamma_{11}$  is suitable to measure the degree of nonplanarity. The intensities of the other ruffling modes observed are less useful to determine this degree because their frequencies are close to those of some A<sub>1g</sub> modes which reveals a pronounced mixing of in- and out-of-plane contributions that varies from one porphyrin to another and therefore obscures the correlation between intensity and porphyrin structure. Similarly to the ruffling inferred from the presence of B<sub>1u</sub> modes for meso-substituted porphyrins, it can be shown that NiOETPP is saddled (B<sub>2u</sub>) in solution. Again, further distortions of other symmetry types cannot be inferred because no lines attributed to B<sub>1u</sub> or A<sub>2u</sub> modes appear in the spectra. Therefore, the conformation in CS<sub>2</sub> or DC is likely close to our predicted structure which is also close to that observed by X-ray diffraction. Further structure information is provided by the depolarization ratio of the Raman line corresponding to the phenyl mode  $\pi_5$ . Its value of  $\approx 0.125$  suggests the phenyl groups to be not perpendicular to the porphyrin plane, as already expected by our molecular mechanics calculation.

Apparently, the result of this study is also relevant for analyzing out-of-plane distortions of heme groups in proteins. Recently, Jentzen et al.<sup>6</sup> have shown by a normal-mode structural decomposition of porphyrins in protein crystals that in particular heme *c* groups in various cytochrome *c* molecules are forced into nonplanar conformations with significant ruffling and saddling. While this is in line with the occurrence of bands assignable to out-of-plane modes in the Raman spectrum of e.g. yeast cytochrome *c*,<sup>26</sup> a quantitative and unambiguous use of this spectral information is outstanding since it requires the calculation of normal coordinates for nonplanar structures of Fe protoporphyrin IX. The situation is similar for heme groups in myoglobin. Hu et al.<sup>27</sup> identified weak but clearly detectable Raman bands from out-of-plane modes in the spectra of deoxyMb, aquomet-, and MbCN. Surprisingly, no conclusions have been drawn from this finding by the authors. Doubtless, the present study provides a sound basis for developing an appropriate force field for this purpose. Even in the present stage, it is usable for identifying Raman bands from ruffling and saddling modes of iron porphyrins since they do not involve motions of the metal itself. With an unambiguous assignment of Raman bands from out-of-plane modes and their normal-coordinate composition at hand, Raman spectroscopists will be able to determine the symmetry of nonplanar distortions. Moreover, by using bands of modes which are not heavily mixed with in-plane vibrations it should be possible to calibrate the corresponding intensities as a quantitative measure of nonplanarity. Thus, for instance, Raman bands from A<sub>2u</sub> modes can be used to monitor changes of heme doming in the relaxation of e.g. heme photoproducts detectable at cryogenic temperatures.

**Acknowledgment.** Work at UC Davis was funded by the National Science Foundation (CHE-96-23117, K.M.S.). C.J.M. acknowledges financial support from Prof. John Shelnuitt (Sandia National Laboratories and University of New Mexico) through the United States Department of Energy. R.J.L. acknowledges a fellowship from the University of Bremen.

## References and Notes

(1) Shelnuitt, J. A.; Song, X.-Z.; Ma, J.G.; Jia, S. L.; Jentzen, W.; Medforth, C. J. *Chem. Soc. Rev.* **1998**, 27, 31.

- (2) (a) Timkovich, R.; Dickerson, R. E. *J. Mol. Chem.* **1976**, 251, 2197. (b) Matsuura, Y.; Takano, T.; Dickerson, R. E. *J. Mol. Biol.* **1982**, 156, 389. (c) Nakagawa, A.; Higuchi, Y. N.; Katsube, Y.; Yagi, T. *J. Biochem (Tokyo)* **1990**, 108, 701. (d) Deisenhofer, J.; Michel, H. *Science* **1989**, 245, 1463. (e) Hobbs, J. D.; Shelnuitt, J. A. *J. Protein Chem.* **1995**, 14, 19. (f) Tronrond, D. E.; Schmid, M. F.; Matthews, B. W. *J. Mol. Biol.* **1986**, 188, 443.
- (3) (a) Schweitzer-Stenner, R. *J. Phys. Chem.* **1994**, 98, 9374. (b) Schweitzer-Stenner, R.; Stichernath, A.; Dreybrodt, W.; Jentzen, W.; Song, X.-Z.; Shelnuitt, J. A.; Faurskov Nielsen, O.; Medforth, C. J.; Smith, K. M. *J. Chem. Phys.* **1997**, 107, 1794. (c) Lemke, C.; Dreybrodt, W.; Shelnuitt, J. A.; Quirke, J. M. E.; Schweitzer-Stenner, R. *J. Raman Spectrosc.* **1998**, 29, 945.
- (4) Shelnuitt, J. A.; Medforth, C. J.; Berber, M. D.; Barkigia, K. M.; Smith, K. M. *J. Am. Chem. Soc.* **1991**, 113, 4077.
- (5) Barkigia, K. M.; Chantranupong, L.; Smith, K. M.; Fajer, J. *J. Am. Chem. Soc.* **1991**, 113, 4077.
- (6) Jentzen, W.; Ma, J.-G.; Shelnuitt, J. A. *Biophys. J.* **1997**, 74, 753.
- (7) (a) Warshel, A. *Proc. Natl. Acad. Sci. USA* **1977**, 74, 1789. (b) Gellin, B. R.; Karplus, M. *Proc. Natl. Acad. Sci. USA* **1977**, 74, 801. (c) LaMar, G. N.; Viscio, D. B.; Smith, K. M.; Caughey, W. S.; Smith, M. L. *J. Am. Chem. Soc.* **1978**, 100, 8084. (d) Ten Eyck, L. F. Hemoglobin and Myoglobin. In *The Porphyrins*; Dolphin, D., Ed.; Academic: New York, 1979; Vol. 3. (e) Schweitzer-Stenner, R. *Q. Rev. Biophys.* **1989**, 22, 381.
- (8) Jentzen, W.; Song, X. Z.; Shelnuitt, J. A. *J. Phys. Chem. B* **1997**, 101, 1684.
- (9) Jentzen, W.; Simpson, M. C.; Hobbs, J. D.; Song, X.; Ema, T.; Nelson, N. Y.; Medforth, C. J.; Smith, K. M.; Veyrat, M.; Mazzanti, M.; Ramasseul, R.; Shelnuitt, J. A. *J. Am. Chem. Soc.* **1995**, 107, 11085.
- (10) Fleischer, E. B.; Miller, C. K.; Webb, L. E. *J. Am. Chem. Soc.* **1964**, 86, 2342.
- (11) McLean, A. L.; Foran, G. J.; Kennedy, B. J.; Turner, P.; Humbley, T. M. *Aust. J. Chem.* **1996**, 49, 1273.
- (12) Jentzen, W.; Unger, E.; Song, X. Z.; Song-Ling, J.; Turowska-Tyrk, I.; Schweitzer-Stenner, R.; Dreybrodt, W.; Scheidt, W. R.; Shelnuitt, J. A. *J. Phys. Chem. A* **1997**, 101, 5789.
- (13) Unger, E.; Dreybrodt, W.; Schweitzer-Stenner, R. *J. Phys. Chem. A* **1997**, 101, 5997.
- (14) (a) Barkigia, K. M.; Berber, M. D.; Fajer, J.; Medforth, C. J.; Renner, M. W.; Smith, K. M. *J. Am. Chem. Soc.* **1990**, 112, 8851. (b) Shelnuitt, J. A.; Majumder, S. A.; Sparks, L. D.; Hobbs, J. D.; Medforth, C. J.; Senge, M. O.; Smith, K. M.; Miura, M.; Luo, L.; Quirke, J. M. E. *J. Raman Spectrosc.* **1992**, 23, 523. (c) Barkigia, K. M.; Renner, M. W.; Furenli, L. R.; Medforth, C. J.; Smith, K. M.; Fajer, J. *J. Am. Chem. Soc.* **1993**, 115, 3627. (d) Sparks, L. D.; Medforth, C. J.; Park, M.-S.; Chamberlain, J. R.; Ondrias, M. R.; Senge, M. O.; Smith, K. M.; Shelnuitt, J. A. *J. Am. Chem. Soc.* **1993**, 115, 581.
- (15) Unger, E.; Lipski, R. J.; Dreybrodt, W.; Schweitzer-Stenner, R. *J. Raman Spectrosc.* **1999**, 30, 3.
- (16) Stichernath, A.; Schweitzer-Stenner, R.; Dreybrodt, W.; Mak, R. S. W.; Li, X.-Y.; Sparks, L. D.; Shelnuitt, J. A.; Medforth, C. J.; Smith, K. M. *J. Phys. Chem.* **1993**, 97, 3701.
- (17) Piffat, C.; Melamed, S.; Spiro, T. G. *J. Phys. Chem.* **1993**, 97, 7441.
- (18) Jentzen, W.; Unger, E.; Karvounis, G.; Shelnuitt, J. A.; Dreybrodt, W.; Schweitzer-Stenner, R. *J. Phys. Chem.* **1996**, 100, 14184.
- (19) Li, X.-Y.; Czernuszewicz, R. S.; Kincaid, J. R.; Su, Y. O.; Spiro, T. G. *J. Phys. Chem.* **1990**, 94, 31.
- (20) Jarzecki, A. A.; Kozlowski, P. M.; Pulay, P.; Ye, B. H.; Li, X.-Y. *Spectrochim. Acta, Part A* **1997**, 1195.
- (21) Jentzen, W.; Turowska-Tyrk, I.; Scheidt, W. R.; Shelnuitt, J. A. *Inorg. Chem.* **1996**, 35, 3559.
- (22) Medforth, C. J.; Muzzi, C. M.; Shea, K. M.; Smith, K. M.; Abraham, R. J.; Jia, S.; Shelnuitt, J. A. *J. Chem. Soc., Perkin Trans.* **1997**, 2, 839.
- (23) Cupane, A.; Leone, M.; Unger, E.; Lemke, C.; Beck, M.; Dreybrodt, W.; Schweitzer-Stenner, R. *J. Phys. Chem. B* **1998**, 102, 6612.
- (24) Li, X.Y. *Resonance Raman Studies and Vibrational Analysis of Nickel Porphyrins*. Ph.D. thesis, Princeton University, Princeton, 1988.
- (25) Li, X. Y.; Czernuszewicz, R. S.; Kincaid, J. R.; Stein, P.; Spiro, T. G. *J. Phys. Chem.* **1990**, 94, 47.
- (26) Hu, S.; Morris, I. K.; Sing, J. P.; Smith, K. M.; Spiro, T. G. *J. Am. Chem. Soc.* **1993**, 115, 12466.
- (27) Hu, S.; Smith, K. M.; Spiro, T. G. *J. Am. Chem. Soc.* **1996**, 118, 12638.
- (28) Pace, L. J.; Martinsen, A.; Ulman, A.; Hoffmann, B. M.; Ibers, J. A. *J. Am. Chem. Soc.* **1983**, 105, 2996.
- (29) Newcomb, T. P.; Godfrey, M. R.; Hoffmann, B. M.; Ibers, J. A. *J. Am. Chem. Soc.* **1989**, 111, 7078.
- (30) Pace, L. J.; Ulman, A.; Ibers, J. A. *Inorg. Chem.* **1982**, 21, 199.
- (31) Newcomb, T. P.; Godfrey, M. R.; Hoffmann, B. M.; Ibers, J. A. *Inorg. Chem.* **1990**, 29, 223.
- (32) Ema, T.; Senge, M. O.; Nelson, N. Y.; Ogoshi, H.; Smith, K. M. *Angew. Chem., Int. Ed. Engl.* **1994**, 33, 1879.